



**HAL**  
open science

# A Blind Reconstruction Algorithm for Level-Crossing Analog-to-Digital Conversion

Antoine Souloumiac

► **To cite this version:**

Antoine Souloumiac. A Blind Reconstruction Algorithm for Level-Crossing Analog-to-Digital Conversion. 2019 27th European Signal Processing Conference (EUSIPCO), Sep 2019, La Coruña, Spain. pp.8902505, 10.23919/EUSIPCO.2019.8902505 . cea-04565715

**HAL Id: cea-04565715**

**<https://cea.hal.science/cea-04565715>**

Submitted on 2 May 2024

**HAL** is a multi-disciplinary open access archive for the deposit and dissemination of scientific research documents, whether they are published or not. The documents may come from teaching and research institutions in France or abroad, or from public or private research centers.

L'archive ouverte pluridisciplinaire **HAL**, est destinée au dépôt et à la diffusion de documents scientifiques de niveau recherche, publiés ou non, émanant des établissements d'enseignement et de recherche français ou étrangers, des laboratoires publics ou privés.

# A Blind Reconstruction Algorithm for Level-Crossing Analog-to-Digital Conversion

Antoine Souloumiac  
CEA LIST

Data Science and Decision Laboratory

CEA Saclay – DIGITEO Saclay, B 565 PC 192, F-91191 Gif-Sur-Yvette Cedex  
antoine.souloumiac@cea.fr

**Abstract**—Many techniques have been developed for spectral analysis and reconstruction of an analog signal based on a nonuniform set of samples. But, to the best of our knowledge, none is specifically adapted to Level-Crossing Analog-to-Digital Converters (LC-ADC). We propose in this article a reconstruction algorithm that takes advantage of the intrinsic quantification of the LC-ADC samples amplitudes to dramatically minimize the stability requirements of the analog levels and improve the converter global accuracy and resolution. We show in particular that spectral analysis is possible even if the levels amplitudes are unknown: they can be blindly estimated, jointly with the signal spectrum, up to harmless indeterminations of scale and offset. Simulations on synthetic signals demonstrate that the proposed algorithm outperforms the existing techniques.

**Index Terms**—Level-Crossing Analog-to-Digital Conversion, Spectral Analysis, Nonuniform Sampling, Reconstruction, Categorical and Mixed Data, Subspaces Intersection, Principal Angles, Singular Value Decomposition.

## I. INTRODUCTION

### A. Nonuniform Sampling and Reconstruction

Let us denote  $x(t)$  the analog signal of interest whose spectral support is assumed limited to the frequency band  $[B_1, B_2]$ ,  $B_1 > 0$  (resp.  $B_1 = 0$ ) if  $x$  is bandpass-limited (resp. low-pass). Any nonuniform sampling technique provides a set  $x(\tau_1), x(\tau_2), \dots, x(\tau_K)$  of samples of  $x(t)$  recorded on the nonuniform time grid  $\tau_1, \tau_2, \dots, \tau_K$ , which means that  $\tau_k - \tau_{k-1}$  depends on  $k$  with  $1 < k \leq K$ . Without loss of generality, we assume that  $0 \leq \tau_1 < \tau_2 < \dots < \tau_K \leq T$  where  $T$  is the length of the observation interval of time  $[0, T]$ .

In many applications nonuniform samples sets cannot be directly used and must be digitally post-processed, or reconstructed. The reconstruction consists in two steps: first estimating the signal spectrum and, second computing a new uniformly sampled set  $\{x(lT_s) \mid 0 \leq l \leq \lfloor T/T_s \rfloor\}$ ,  $1/T_s$  being the new reconstruction sampling frequency. This article is mainly devoted to the spectral estimation of nonuniformly sampled band-limited analog signals. The new samples computation step is straightforward (and optional in some applications) and it will only be used here to illustrate the algorithms performance.

The author thanks Marine Depecker-Quéchon for fruitful discussion on mixed data that has triggered this research.

### B. Spectral Analysis on a finite interval of time

The signal  $x(t)$  being observed only in the interval  $[0, T]$ , we consider its  $T$ -periodic version denoted  $x_p(t)$  and defined by  $x_p(t) \stackrel{\text{def}}{=} x(t - \lfloor t/T \rfloor \times T)$ . The  $x_p(t)$  has a discrete spectrum and can be represented by its corresponding Fourier series. But it must be noted that  $x_p(t)$  and  $x(t)$  spectra are not exactly equal. As a matter of fact, the periodization yields a discrete spectrum at the price of a convolution by a *sinc* function of width  $1/T$  which widens the band-limited spectrum of  $x(t)$ .

Nevertheless, this distortion can be reduced by choosing  $T$  large enough so that  $1/T$  is small compared to  $B_1$  (if  $B_1 > 0$ ) and  $B_2$ . In addition, the spectrum widening can be partially taken into account by increasing  $B_2$  by a small multiple of  $1/T$  and decreasing  $B_1$ , when  $B_1 > 0$ , by the same quantity. The difference between  $x$  and  $x_p$  spectra will be neglected in the rest of this article like in [2], [5] for instance, and the notation  $x_p$  will not be used any further. To summarize, the analog signal of interest  $x(t)$  is considered accurately approximated by a truncated Fourier series (see below Eq. 2) that is to be used to reconstruct any sample  $x(t)$  with  $t \in [0, T]$ .

### C. Level-Crossing Analog-to-Digital Conversion

Standard Analog-to-Digital Conversion (ADC) consists in measuring the signal amplitude at given sampling instants which generally constitute a uniform time grid. In Level-Crossing ADC (LC-ADC) time and amplitude are interchanged: time moments are measured when the signal crosses given levels or thresholds which constitute a fixed amplitude grid. The fixed time grid of standard ADC is replaced by an fixed amplitude grid, as illustrated in Fig. 1.

The main advantage of LC-ADC is that it is easier to measure accurately a time instant than an analog amplitude. In practice, the LC-ADC analog electronics reduces to a reference voltage and a comparator for each threshold combined to a fast clock and a device to count and record the numbers of clock ticks between every pairs of successive threshold crossings. In comparison, the analog architecture of standard ADCs, e.g. flash, successive approximation or even Sigma-Delta, is much more complex. In addition, LC-ADC necessitate very few thresholds: in this article we only consider ADC with less than ten thresholds, even when converting large bandwidth

signals. Several authors investigated LC-ADC with only one zero-threshold – i.e. zero-crossings systems – see for instance [1] or the bibliography in [6].

Besides, the (few) thresholds amplitudes can be optimized in different ways: a nonuniform distribution increases the ADC dynamic range and equalizes the signal-to-noise ratio [5], or no thresholds in a range of amplitudes where the signal is considered as noninformative (close to zero for instance) prevents many useless conversions (and the corresponding consumption). Of course, the LC-ADC clock speed must be much larger than the signal of interest highest frequency but this does not limit LC-ADC to very low frequency signals as demonstrated for instance in [5] which investigates an application to 10 megahertz ultrasound signals with a 100 gigahertz clock. All these advantages allow to build very low consumption converters particularly relevant for embedded systems [5]. In summary, LC-ADC reduces the analog electronics requirements in comparison to standard ADCs at the price of the additional digital reconstruction step, which allows to use the advantages of digital systems like on-the-fly reconfigurations of the frequency band among others.

### D. Spectral Analysis with a Level-Crossing ADC

As said above, any (analog) nonuniform sampling device provides the samples moments  $\tau_k$  and the amplitudes  $x(\tau_k)$  that are processed in the (digital) spectral analysis step, see [2] or the bibliography in [5]. However the LC-ADC samples amplitudes are by construction equal to the (few) thresholds amplitudes i.e. several analog reference voltages that cannot be expected to be perfectly stable over time. Calibrations could allow to follow the thresholds drifts but they are costly or even impossible in embedded systems. Therefore, the thresholds (and the samples) amplitudes cannot be known exactly in practice, which strongly decreases the LC-ADC global accuracy as it will be illustrated below.

Nevertheless, it is reasonable to assume that the thresholds amplitudes deviations are as slow as the dynamic of physical phenomena at stake, like temperature drift and/or components aging for instance. The proposed reconstruction algorithm for LC-ADC is based on the realistic assumption that the thresholds levels are unknown but constant during short observation intervals of time  $[0, T]$  (only contexts with  $T$  shorter than 1 minute are considered here for instance).

In the next section, we show how the few thresholds amplitudes AND the signal spectrum (the Fourier coefficients) can be jointly estimated up to some unavoidable indeterminations (scale and possibly offset). But these indeterminations can be later reduced using the available information about thresholds amplitudes when it is required by the application in view, see section II-F. This is a blind reconstruction technique because some uncertain a priori information (the thresholds amplitudes here) is ignored when estimating the analog signal spectrum. In the third section we compare the accuracy of the proposed technique with the standard Adaptive-weights Conjugate-gradients Toeplitz (ACT) algorithm [2] on synthetic signals. We show in particular the sensitiveness of existing

methods to thresholds amplitudes uncertainty. This article generalizes previous results in [7], [8] to low-pass signals and to multidimensional intersection modes.

## II. BLIND SPECTRAL ESTIMATION ALGORITHM

### A. The Thresholds Crossings Information

Let us denote  $M$  the number of thresholds and  $y \stackrel{\text{def}}{=} (y_1, y_2, \dots, y_m, \dots, y_M)^T$  the vector of the thresholds amplitudes. As already said, the signal of interest  $x(t)$  crosses the  $M$  thresholds at the  $K$  times  $\tau_1, \tau_2, \dots, \tau_K$  in the observation interval of time  $[0, T]$ . We define the function  $\mu$  from  $\{1, 2, \dots, K\}$  to  $\{1, 2, \dots, M\}$  such that  $\mu(k) = m$  if  $x(\tau_k) = y_m$ : in other words  $\mu$  maps each crossing time index  $k$  to the index  $m$  of the threshold  $y_m$  actually crossed at time  $\tau_k$ . The vector of signal amplitudes  $(x(\tau_1), x(\tau_2), \dots, x(\tau_K))^T$  is denoted  $x$  and

$$x \stackrel{\text{def}}{=} \begin{pmatrix} x(\tau_1) \\ x(\tau_2) \\ \vdots \\ x(\tau_k) \\ \vdots \\ x(\tau_K) \end{pmatrix} = \begin{pmatrix} y_{\mu(1)} \\ y_{\mu(2)} \\ \vdots \\ y_{\mu(k)} \\ \vdots \\ y_{\mu(K)} \end{pmatrix} = C \begin{pmatrix} y_1 \\ y_2 \\ \vdots \\ y_M \end{pmatrix} \stackrel{\text{def}}{=} Cy \quad (1)$$

where  $C$  is a  $K \times M$  binary matrix such that  $C(k, m) = 1$  if  $m = \mu(k)$  and  $C(k, m) = 0$  otherwise. Note that  $C$  is the binary matrix classically associated by one-hot coding to any categorical data like  $\mu(k)$ .  $C$  has exactly one 1 on each row, its columns are orthogonal and non-zero when discarding uncrossed thresholds.

In practice, the duration of the observation interval  $T$  is chosen long enough so that there are much more thresholds crossings than thresholds ( $K \gg M$ ) i.e.  $C$  has more rows than columns. The  $M$ -dimensional linear subspace generated by the  $M$  columns of  $C$  is denoted  $\text{Span}(C)$ , and,  $y$  being unknown, (1) simply means  $x \in \text{Span}(C)$ . Note that the loss of all information about the thresholds amplitudes  $y$  induces a remarkable reduction of information about  $x$ : in the blind context we do not know exactly  $x$  but only that  $x$  belongs to a  $M$ -dimensional subspace. Nevertheless this remaining subspace information allows surprisingly accurate reconstructions.

### B. The Spectral Information

As mentioned in I-B, the band-limited signal  $x(t)$  is represented by a truncated Fourier series

$$x(t) = \sum_{n=1}^{n=N} p_n \cos(2\pi f_n t) + q_n \sin(2\pi f_n t) \quad (2)$$

where a possible choice of the frequencies is  $f_n = B_1 + (n - 1)/T$  and  $N = \lceil (B_2 - B_1)T \rceil$ . (In the case of a low-pass signal of interest  $x(t)$ , i.e. when  $B_1 = 0$  and  $f_1 = 0$ , (2) is to be understood without the  $q_1$  term.) The discrete and finite spectrum  $X$  of the analog signal  $x(t)$  is defined as the vector of its Fourier coefficients  $X \stackrel{\text{def}}{=} (\dots p_n \dots, \dots q_n \dots)^T$ .

If we denote  $F$  the  $K \times 2N$  matrix ( $K \times (2N - 1)$  in the low-pass context)

$$F \stackrel{\text{def}}{=} \begin{pmatrix} \dots & \cos(2\pi f_n \tau_1) & \dots & \sin(2\pi f_n \tau_1) & \dots \\ & \vdots & & \vdots & \\ \dots & \cos(2\pi f_n \tau_k) & \dots & \sin(2\pi f_n \tau_k) & \dots \\ & \vdots & & \vdots & \\ \dots & \cos(2\pi f_n \tau_K) & \dots & \sin(2\pi f_n \tau_K) & \dots \end{pmatrix} \quad (3)$$

and apply (2) to the  $K$  crossing moments  $\tau_1, \tau_2, \dots, \tau_K$  then the vector of samples  $x$ , the matrix  $F$  and the spectrum  $X$  of the signal  $x(t)$  are related by the linear relation  $x = FX$ .

As illustrated in the next section, the duration  $T$  of the observation interval and the number  $M$  of thresholds can be chosen large enough so that the number of crossings  $K$  is larger than the number of Fourier coefficients  $2N$  (or  $2N - 1$  in the low-pass case). The matrix  $F$  has more rows than columns and its columns span a  $2N$ -dimensional linear subspace denoted  $\text{Span}(F)$  and,  $X$  being unknown,  $x = FX$  can be interpreted as  $x \in \text{Span}(F)$ . Note that this argumentation is not as straightforward as in II-A because the number of frequencies  $N$  grows linearly with  $T$ .

### C. Standard Reconstruction

The standard reconstruction techniques compute the unknown spectrum  $X$  via a least squares minimization of the error term  $FX - x$  i.e. solving a linear system equivalent to  $F^T FX = F^T x$ . In practice the matrix  $F$ , and a fortiori  $F^T F$ , are generally large and extremely ill-conditioned and solving such a system is numerically difficult. The ACT algorithm [2] uses a weighted conjugate gradient algorithm to deal with large systems involving hundreds of frequencies ( $N$ ) and thousands of crossing ( $K$ ). In the case of the LC-ADC such an approach is not accurate because the thresholds amplitudes  $y$ , i.e. the entries of  $x$ , are not known exactly in practice, and – even small – errors on  $x$  are strongly amplified.

### D. The Proposed Algorithm

If we ignore any a priori information about the thresholds amplitudes then the LC-ADC only provides the indices  $\mu(1), \mu(2), \dots, \mu(K)$  of the crossed thresholds (categorical data) and the crossing moments  $\tau_1, \tau_2, \dots, \tau_K$  (numerical data). The indices allow to compute the matrix  $C$  and the crossing moments combined with the set of frequencies  $f_1, f_2, \dots, f_N$  allow to compute the matrix  $F$ . As seen previously,  $x$  belongs to  $\text{Span}(C)$  and  $\text{Span}(F)$  therefore it belongs to their intersection

$$x \in \text{Span}(C) \cap \text{Span}(F) \quad (4)$$

Of course this characterization of  $x$ , and consequently of  $y$  and  $X$ , is of interest only if the dimension of  $\text{Span}(C) \cap \text{Span}(F)$  is very small. Conditions are given in the next section to guarantee that the intersection dimension  $p$  is equal to 1 or 2 ( $p = 1$  corresponds to a scale indetermination,  $p = 2$  to offset and scale indeterminations). This algorithm is called TSSIRA for Two SubSpaces Intersection Reconstruction Algorithm.

The practical computation of the intersection of two linear subspaces is standard, see for instance the algorithm 12.4.3, page 604 in [3]. First orthonormal bases of the two subspaces are to be computed via (“economy size”) QR decompositions of  $C$  and  $F$  (an SVD could also be used)

$$C = Q_C R_C \quad \text{and} \quad F = Q_F R_F \quad (5)$$

Second the (“economy size”) singular value decomposition of the  $2N \times M$  matrix  $Q_F^T Q_C$  is computed and denoted  $U \Sigma V^T$ . The singular values in  $\Sigma$  are the cosines of the principal angles between the two subspaces: if the  $p$  largest singular values  $\sigma_1, \dots, \sigma_p$  are equal to 1 and  $\sigma_{p+1} < 1$  then the intersection is  $p$ -dimensional. If we denote  $U_1$  (resp.  $V_1$ ) the  $2N \times p$  matrix of left (resp. the  $M \times p$  matrix of right) singular vectors corresponding to the singular value 1 then we have

$$x = Q_F R_F X \in \text{Span}(Q_F U_1) \quad \text{and} \quad (6)$$

$$x = Q_C R_C y \in \text{Span}(Q_C V_1) \quad (7)$$

and the solution to the blind reconstruction problem is

$$X \in \text{Span}(R_F^{-1} U_1) \quad \text{and} \quad y \in \text{Span}(R_C^{-1} V_1) \quad (8)$$

### E. Practical Remarks

One must first note that the scale indetermination is intrinsic to any subspace intersection method; it corresponds to the invariance of the crossing moments when scaling both the signal and the thresholds. The question is: how to choose the duration  $T$  of observation and the number  $M$  of thresholds in function of the signal frequency band  $[B_1, B_2]$  to guarantee an intersection of dimension 1 or 2, and thus limit the indeterminations to scale and offset. This theoretical problem is difficult because they are no closed form expression of the singular values of  $Q_F^T Q_C$ , or the principal angles between  $\text{Span}(C)$  and  $\text{Span}(F)$ , as functions of  $B_1, B_2, T$ , etc. Therefore we only provide here rules based on empirically observations.

In the bandpass case, we noticed that  $T \approx 10/B_1$  is a convenient minimal duration of observation (the intuition is to observe at least 10 of the longest period present in  $x(t)$ ). With that value of  $T$ , the number of thresholds can be tuned with respect to  $\beta \stackrel{\text{def}}{=} B_2/B_1$ : in the simulations we used typically  $(M, \beta) = (2, 4), (4, 30), (8, 100)$  and  $(10, 300)$ . In these conditions the blind problem solution is 1-dimensional and there is only a scale indetermination. When  $T$  is shorter, e.g.  $T \approx 1/B_1$ , the blind solution is 2-dimensional because the constant vector  $(1, 1, \dots, 1)^T$ , that belongs by construction to  $\text{Span}(C)$ , also belongs to  $\text{Span}(F)$  and consequently to their intersection. This vector generates an offset indetermination on top of the scale one.

In the more difficult low-pass context, the first column of  $F$  is by definition equal to the constant vector: the minimal dimension of the blind problem solution is necessarily 2 and the corresponding scale and offset indeterminations are unavoidable. The  $T$  lower bound cannot obviously be a function of  $B_1 = 0$  and depends on the actual spectrum of  $x(t)$ . In our simulations, the spectrum is approximately flat (sinewaves frequencies are uniformly distributed on  $[0, B_2]$ ) and the

conditions  $T \approx 10/B_2$  and  $M = 10$  seems to guarantee enough thresholds crossings for accurate reconstruction.

The TSSIRA algorithm has many additional practical advantages for monitoring the LC-ADC. The largest singular value  $\sigma_1$  – in  $[0, 1]$  by construction – is generally very close to 1. A value of  $\sigma_1$  too far from 1 allows the online detection of a model error like an erroneous frequency band or a circuit nonlinearity. The TSSIRA algorithm also provides the thresholds amplitudes whose drifts can be monitored (up to the indeterminations) during long periods of time. Parameters can be tuned e.g. the distance between successive frequencies  $f_n$  can be slightly lower than  $1/T$  as done in the simulations below.

### F. Treatment of the Indeterminations

In many applications like communications, the scale and offset indeterminations do not alter the information carried by the signal, nevertheless a rough estimation of the actual signal range may be of practical use. The goal is only to fix the  $p = 1$  or  $p = 2$  degrees of freedom that remain free after solving the blind reconstruction problem. In practice, the thresholds amplitudes  $y$  are always known approximately (at least their order of magnitude) and that available a priori information is sufficient to select one solution in the  $p$ -dimensional subspace  $\text{Span}(R_C^{-1}V_1)$ .

Concretely, one can choose a vector  $y$  in  $\text{Span}(R_C^{-1}V_1)$  that is as close as possible to the ADC thresholds nominal values  $y_0$ , or the  $y$  vector such that  $p$  specific thresholds have the expected amplitude (e.g. the maximal threshold if  $p = 1$ , and the minimal and maximal thresholds if  $p = 2$ ). Blind LC-ADC can address metrology applications if (only) 1 or 2 thresholds have very accurate and stable amplitudes, which reduces dramatically the usual constraints on the whole set of  $M$  thresholds. Whatever the selection procedure may be, the selected vector  $y_s$  is finally characterized by a  $p$ -dimensional vector  $\alpha$  such that  $y_s = R_C^{-1}V_1\alpha$  that, after some simple algebra, gives also the selected spectrum  $X_s = R_F^{-1}U_1\alpha$  and finally any desired sample  $x(t)$  of the signal of interest when  $t \in [0, T]$  by using (2).

## III. EVALUATION OF PERFORMANCE

### A. Generation of the Input Synthetic Data

The band-limited analog signal is generated as the sum of many sinewaves (much more than  $2N$ ) of random frequencies in the band  $[B_1 = 1 \text{ hz}, B_2]$  and random amplitudes and phases. Thus, any sample of the signal or its time derivative can be computed exactly. The thresholds amplitudes are exponentially distributed in the analog signal range like in Fig. 1. This context is of course favorable: the thresholds numbers used here are to be understood as the minimal ones. When the signal range is unknown, it is necessary to use larger numbers of thresholds and select the most informative (crossed) ones to reduce the size of  $C$  and  $F$  and the reconstruction numerical complexity. In our simulations, the thresholds crossings moments are efficiently computed using few tens of Newton iterations with an accuracy better than  $10^{-11}$  second even with

more than  $10^4$  crossings. This maximal initial accuracy is then digitally reduced to larger values like  $10^{-9}$  or  $10^{-6}$  second to model high but limited clock frequencies  $F_{CLK} = 1/T_{CLK}$ .

### B. Low-pass Signal

Fig. 1 illustrates the principle of LC-ADC reconstruction of a low-pass signal with an observation of 50 seconds: initial (blue) and reconstructed (red) signals are not discernible.

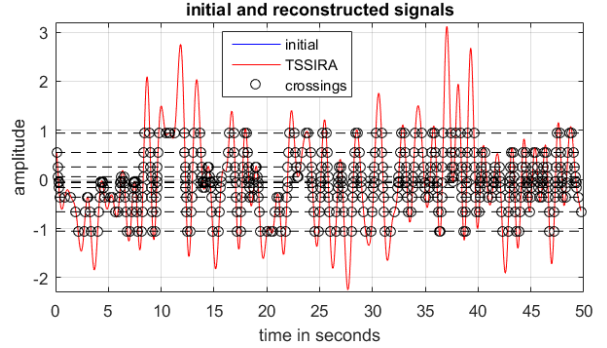


Fig. 1.  $[0, 1]$  hertz low-pass signal,  $N = 59$  frequencies,  $M = 10$  thresholds,  $K = 462$  crossings,  $\sigma_{1,2,3} = 1, 1, 0.71$ .

The reconstruction accuracy of the TSIRRA blind algorithm is shown on Fig. 2 as a function of time: the error is below  $10^{-4}$  except in the first and last seconds of observation.

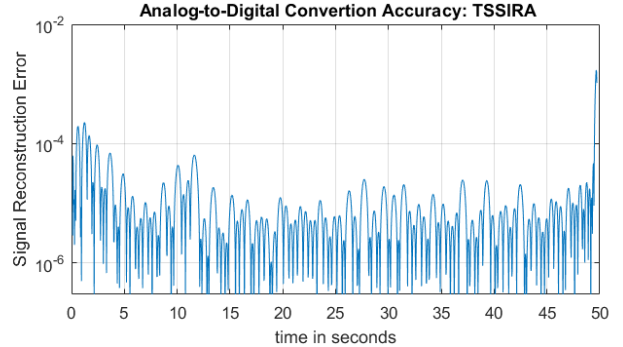


Fig. 2.  $[0, 1]$  hertz low-pass signal,  $N = 59$  frequencies,  $M = 10$  thresholds,  $K = 462$  crossings,  $\sigma_{1,2,3} = 1, 1, 0.71$ .

### C. Bandpass Signal

The impact of the LC-ADC clock is evaluated on analog signals in  $[1, 100]$  hertz observed during  $T = 2$  seconds (2D intersection) and  $T = 10$  seconds (1D intersection). In the first context Fig. 3 (resp. second context Fig. 4) the crossing moments are rounded with the three clock periods:  $T_{CLK} = 10^{-5}, 10^{-6}, 10^{-7}$  seconds (resp.  $T_{CLK} = 10^{-4}, 10^{-6}, 10^{-8}$  seconds). The scale and offset indeterminations (resp. scale only) are reduced using the exact knowledge of the maximum and minimum thresholds amplitudes (resp. the maximum threshold amplitude). The clock frequency i.e. the crossing moments measurement accuracy is clearly the key parameter.

To assess the improvement of the proposed algorithm, we show in Fig. 5 the accuracy obtained using the ACT algorithm

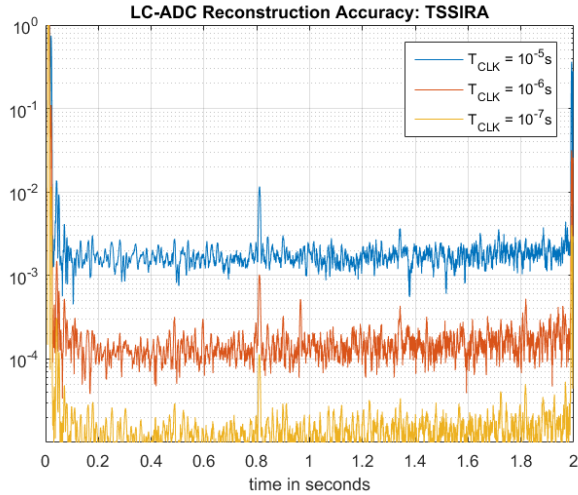


Fig. 3. [1, 100] hertz bandpass signal,  $N = 238$  frequencies,  $M = 10$  thresholds,  $K = 1100$  crossings,  $\sigma_{1,2,3} = 1, 1, 0.896$ .

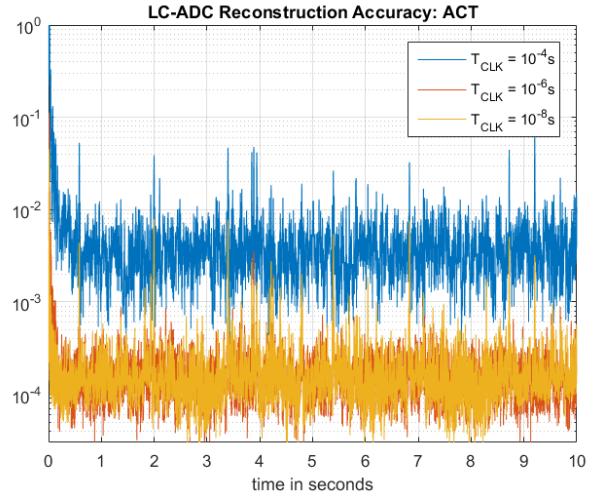


Fig. 5. [1, 100] hertz bandpass signal,  $N = 1188$  frequencies,  $M = 10$  thresholds,  $K = 5550$  crossings,  $\Delta y = 10^{-4}$ .

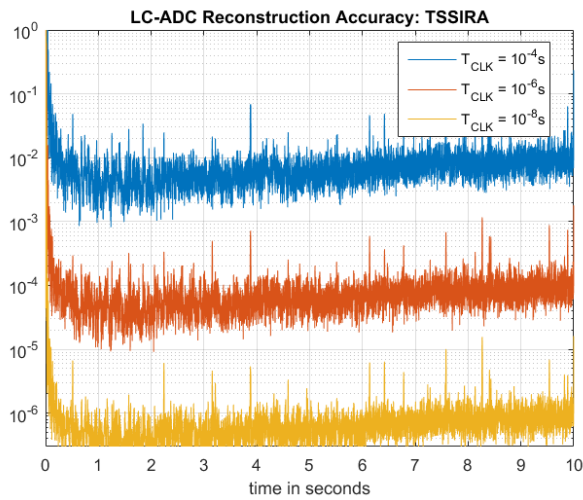


Fig. 4. [1, 100] hertz bandpass signal,  $N = 1188$  frequencies,  $M = 10$  thresholds,  $K = 5550$  crossings,  $\sigma_{1,2,3} = 1, 0.98, 0.88$ .

when the  $M = 10$  thresholds amplitudes are modified by a zeromean Gaussian noise of very small standard deviation  $\Delta y = 10^{-4}$ . The reconstruction accuracy that is similar to the TSSIRA one (Fig. 4) when the thresholds are known exactly ( $\Delta y = 0$ ) is now dramatically reduced to roughly the level of the uncertainty of the thresholds. A test (not shown here due to lack of space) with a more realistic  $\Delta y = 10^{-2}$  uncertainty on the thresholds amplitudes yields a reconstruction error larger than  $10^{-2}$ .

#### IV. CONCLUSION

Existing reconstruction algorithms after LC-ADC nonuniform sampling are extremely sensitive to an uncertainty on the thresholds amplitudes that is unavoidable in practice. The proposed algorithm solves the blind problem exploiting as much as possible the accurate data, i.e. the crossed thresholds

indices and crossings moments, and selects in the blind problem set of solutions a spectrum compatible with the available information about inaccurate data (thresholds amplitudes). Empirical conditions on the duration of the sampling interval, the number of thresholds and the signal bandwidth are given for very accurate reconstruction up to harmless indeterminations of scale and possibly of offset. This study has to be completed by a theoretical investigation of the subspaces intersection dimension, a correction method of the analog comparators timing imperfections, an optimal weighting of each level crossing like in ACT, an online extension of the batch reconstruction algorithm described here, and finally a validation with a hardware implementation.

#### REFERENCES

- [1] S. Kay et R. Sudhaker, "A Zero Crossing-Based Spectrum Analyzer," *IEEE Trans. on Acoustics, Speech, and Signal Processing*, vol. 34, n. 1, pp. 96-104, February 1986.
- [2] H. G. Feichtinger, K. Gröhenig et T. Strohmer, "Efficient Numerical Methods in non-Uniform Sampling Theory," *Numer. Math.*, vol. 69, n. 4, pp. 423-440, 1995.
- [3] G. Golub et C. Van Loan, "Matrix Computations, 3rd edition," The Johns Hopkins University Press, 1996.
- [4] N. Sayiner, H. V. Sorensen et T. R. Viswanathan, "A Level-Crossing Sampling Scheme for A/D Conversion," *IEEE Trans. on Circuits and Systems II: Analog and Digital Signal Processing*, vol. 43, n. 4, pp. 335-339, April 1996.
- [5] K. Kozmin, J. Johansson et J. Delsing, "Level-Crossing ADC Performance Evaluation Toward Ultrasound Application," *IEEE Trans. on Circuits and Systems I: Regular Papers*, vol. 56, n. 8, pp. 1708-1719, August 2009.
- [6] R. Kumaresan et N. Panchal, "Encoding Bandpass Signals Using Zero/Level Crossings: A Model-Based Approach," *IEEE Trans. on Audio, Speech, and Language Processing*, vol. 18, n. 1, pp. 17-33, January 2010.
- [7] A. Souloumiac, "Method and device for measuring the spectrum of an analogue signal, and analogue-digital converter," Patent WO2018069021 (A1), 12 October 2016.
- [8] A. Souloumiac, "Caractérisation d'un signal passe-bande par datation d'instant de franchissement de seuils inconnus," in *Proceedings XXVleme Colloque Gretsi, Juan-Les-Pins, France, September 2017*.